Synthesis, structure and electrochemical behaviour of Ru(II)- and Pt(II)-carbene complexes of the NCN-pincer 1,3-bis(2-pyridylmethyl)-1*H*-benzimidazolium chloride†

Sirsendu Das Adhikary,[a] Tapastaru Samanta,[a] Gourisankar Roymahapatra,[a] Frédérique Loiseau,[b] Damien Jouvenot,[b] Santanab Giri,[c] Pratim K. Chattaraj[c] and Joydev Dinda*[a]

Received (in Victoria, Australia) 23rd November 2009, Accepted 22nd March 2010
DOI: 10.1039/b9nj00698b

Novel NCN-pincer carbene complexes of Ru(II), 1,3-bis(2-pyridylmethyl)-benzimidazolineruthenium(II) bishexafluorophosphate (**2**), and Pt(II), 1,3-bis(2-pyridylmethyl)benzimidazolinechloroplatinum(II) hexafluorophosphate (**3**), complexes based on 1,3-bis(2-pyridylmethyl)-1*H*-benzimidazolium chloride (**1**) were synthesized and characterized by different spectroscopic methods. Complex **2** shows an absorption maximum at 386 nm, blue-shifted in comparison to $Ru(bpy)_3^{2+}$ and $Ru(tpy)_2^{2+}$, probably due to the strong σ-donor and weak π-acceptor properties of the electron-rich NHC ligand. Electrochemical studies show Ru(II)/Ru(III) and Pt(II)/Pt(IV) reversible couples at 0.67 and 0.58 eV, respectively, lower than those for the analogous complexes of ligands like bipyridine (bpy), terpyridine (tpy) and phenylbipyridine (pbpy). The solid state structure of **2** was solved by X-ray diffraction. Theoretical studies (B3LYP/LANL2DZ) of the complex show a HOMO (−0.38594 au) mainly centered on the ruthenium and benzimidazole, whereas the LUMO (−0.25130 au) is populated by pyridines. Therefore, it is assumed that the charge transfer from HOMO → LUMO is mixed ILCT (interligand charge transfer)/MLCT (metal to ligand charge transfer). The observed lower redox potentials of the Pt(II) complex compared to the Ru(II) complex is supported by theoretically calculated ionisation potentials and also electron affinity values. To the best of our knowledge, **2** is the first example of a six-membered metallacycle homoleptic chelate pincer NCN–Ru(II) *N*-heterocyclic carbene complex.

Introduction

Ever since the first successful isolation of a stable *N*-heterocyclic carbene (NHC) by Arduengo,[1] there has been immense growth in the field of NHC chemistry over the last couple of decades.[2] NHCs are attracting great attention as alternatives to phosphines, even becoming more credible than phosphines,[3] in homogeneous catalysis,[4] and becoming versatile ligands in organometallic and inorganic chemistry.[5] Because of their specific coordination motif by a "push–pull" mechanism, NHCs can stabilize and activate metal centers and are excellent in catalysis.[6] New catalysts are being discovered frequently,[7] with structural and functional diversities[8] being introduced into the NHC to modify their catalytic activity.[8c–e] In this regard, chelation plays an important role in the electronic properties[9] of the metal, thus modifying its catalytic and photoelectronic properties. Moreover, *N*-heterocyclic pincer carbene ligands[10] are among the most attractive derivatives because of their highly entropic chelate effect, thus providing a new family of highly stable compounds with interesting chemical properties. In the literature, there are examples of pyridine-, lutidine- and xylyl-bridged pincer ligands of imidazole and benzimidazole with CNC, CCC and NCN binding motifs (Chart 1).[11] For catalysis purposes, Cr,[12a,b] Pd,[11b–d,12c] Fe,[12d,e] Ni,[12f] Co,[12g,h], Ru,[12i–m] *etc.*, metal complexes of pincer ligands have been largely studied. On the other hand, Ru(II) complexes have been studied for photoluminescence[13] as their coordination environment is comparable to $Ru(tpy)_2^{2+}$. The photoluminescence and electrochemical properties of Ru(II) and Pt(II) have been scarcely studied in the case of NHC pincer complexes, though they could be potential candidates for the chromophoric components in light-emitting devices, artificial photosynthesis mimics or light-emitting sensors.[14] Even if $Ru(tpy)_2^{2+}$ displays poor luminescence and short excited state lifetimes at room temperature in comparison to $Ru(bpy)_3^{2+}$, structural modifications[15] can be applied to design new NHC terpyridine analogs featuring the desired properties.

[a] *School of Applied Science, Applied Synthetic Chemical Research Laboratory, Haldia Institute of Technology, Haldia 721657, Purba Medinipur, West Bengal, India. E-mail: dindajoy@yahoo.com; Fax: +91-3224-252800; Tel: +91-9733058113*
[b] *Département de Chimie Moléculaire, UMR CNRS 5250, ICMG – FR 2607, Université Joseph Fourier, BP-53, 38041 Grenoble Cedex 9, France*
[c] *Department of Chemistry and Center for Theoretical Studies, Indian Institute of Technology Kharagpur, Kharagpur 721302, India*

† CCDC reference number 771107. For crystallographic data in CIF or other electronic format see DOI: 10.1039/b9nj00698b

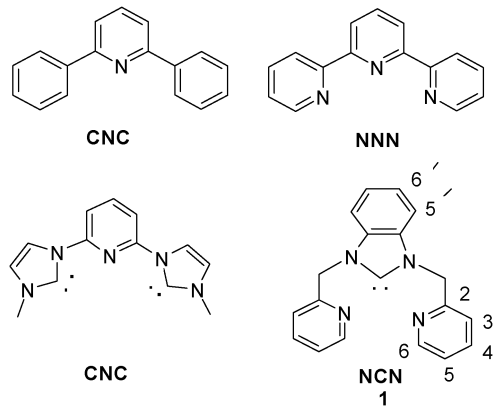

Chart 1

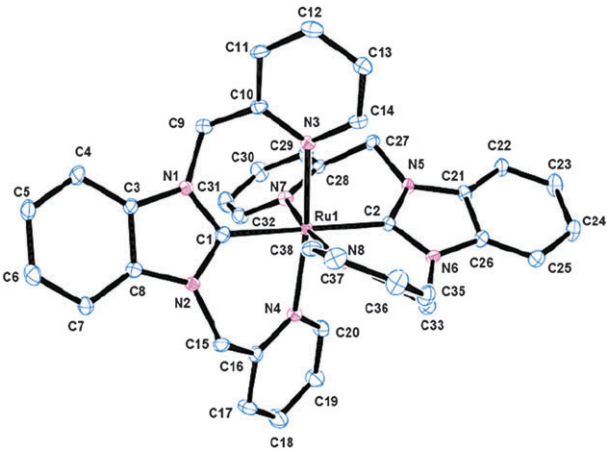

Fig. 1 An ORTEP view of the single crystal X-ray structure of Ru(II) complex **2** (20% probability) (hydrogen atoms, the PF_6 ion and three half-occupancy MeCN molecules have been removed for clarity).

Results and discussion

Synthesis of ligand 1, Ru(II) complex 2 and Pt(II) complex 3

The synthesis of the benzimidazolium-bridged picolylchloride ligand 1,3-bis(2-pyridylmethyl)-1*H*-benzimidazolium chloride (**1**) followed a reported procedure (Scheme 1);[16] the yield was 75%. The corresponding tridentate homoleptic Ru(II) complex, **2**, was prepared according to another literature procedure.[13c] After column purification, the yellow compound was obtained in 65% yield. Crystals suitable for X-ray analysis were obtained from the slow diffusion of diethylether into an acetonitrile solution of the complex (Fig. 1).

The square planar Pt(II) complex 1,3-bis(2-pyridylmethyl)-benzimidazolineplatinum(II) chlorohexafluorophosphate (**3**) was synthesized by the silver carbene transfer method.[17] One equivalent of ligand **1** and 0.5 equivalents of Ag_2O were taken into DMSO and stirred for 36 h, followed by the addition of K_2PtCl_4 in DMSO. The counteranion was exchanged from Cl^- to PF_6^- and product isolated by a reported procedure;[17e] the yield was 75%.

The ^1H NMR spectrum of ligand **1** exhibits a singlet for the procarbenic proton at 9.83 ppm. This value is within the range observed for related benzimidazolium salts.[11d–f] The resonance of the methylene proton appears as a singlet at 5.91 ppm, which is in agreement with that recently reported for the Br^- salt of ligand **1**. The formation of the benzimidazolium salt was also evidenced by the appearance of the NCN resonance at 155 ppm in the ^{13}C NMR spectrum. In the case of Ru(II) complex **2**, the absence of the NCN benzimidazolium proton of the free ligand and the downfield shift of the aromatic protons confirms its formation. Strong chelation through the pyridine N-atom is supported by the appearance of a multiplet at 7.91 ppm for the C_4 proton *trans* to the pyridine N-atom. As expected, the methylene protons show a characteristic AB-type doublet at 5.88 and 4.79 ppm, indicating the diastereotopic nature of these protons once the ligand is coordinated. The ^1H NMR spectrum of Pt(II) complex **3** slightly differs from the

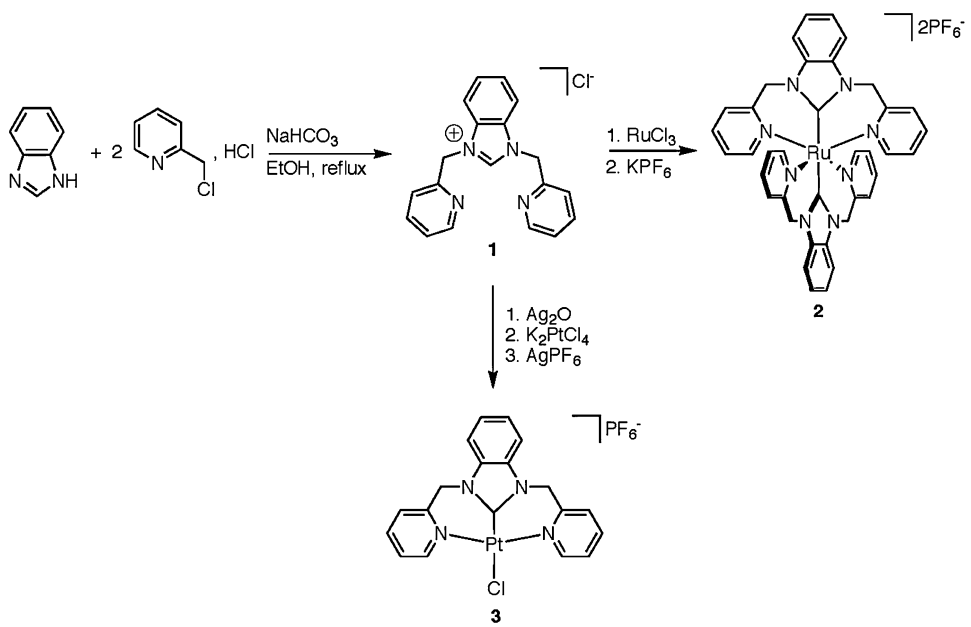

Scheme 1 Synthesis of ligand **1**, Ru(II) complex **2** and Pt(II) complex **3**.

one of Ru(II) complex **2**. The main difference in the ^{1}H NMR spectrum of complex **3** is the quite downfield chemical shift observed for proton C6 (9.64 ppm). This phenomenon is explained by the fact that in complex **2**, this proton is strongly affected by the ring current produced by the facing ligand and is therefore largely shielded. The ring current effect disappears in the case of complex **3**, where proton C6 is now facing the chloro ligand. In a similar way, complex **3** also displays an AB-type doublet at 5.93 and 4.85 ppm, attributed to the diastereotopic effect of the bridging methylene protons. The downfield shift (to 7.57 ppm in the case of **3** and 6.68 ppm in the case of **2**) of the phenyl proton of the benzimidazole indicates a strong inductive effect by Pt(II).

Complexes **2** and **3** are non-emissive in acetonitrile at room temperature. Complex **2** shows an absorption maximum at 386 nm, blue shifted in comparison to $Ru(bpy)_3^{2+}$ and $Ru(tpy)_2^{2+}$ due to strong σ-donor and weak π-acceptor properties, and a smaller aromatic system of the electron-rich NHC ligand compared to the bpy and tpy ligands. Indeed, the NHC ligand has a higher electron density than bpy, tpy or pbpy, and the energy level of the π* orbital (LUMO) is higher. Therefore, the HOMO–LUMO energy gap of **2** and **3** is higher than analogous complexes of bpy, tpy or pbpy (Fig. 2 and Fig. 3). This behaviour is also observed in the case of complex **3**, which exhibits an absorption maximum at 368 nm, blue shifted in comparison with the [Pt(pbpy)Cl]Cl analogue (pbpy = 6-phenyl-2,2′-bipyridine) containing a CNN donor.[14b–d]

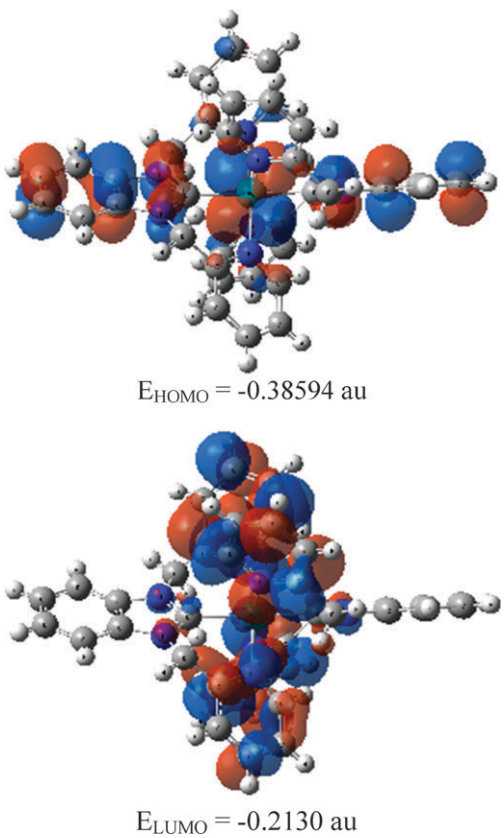

Fig. 2 The HOMO–LUMO orbitals of Ru(II) complex **2**.

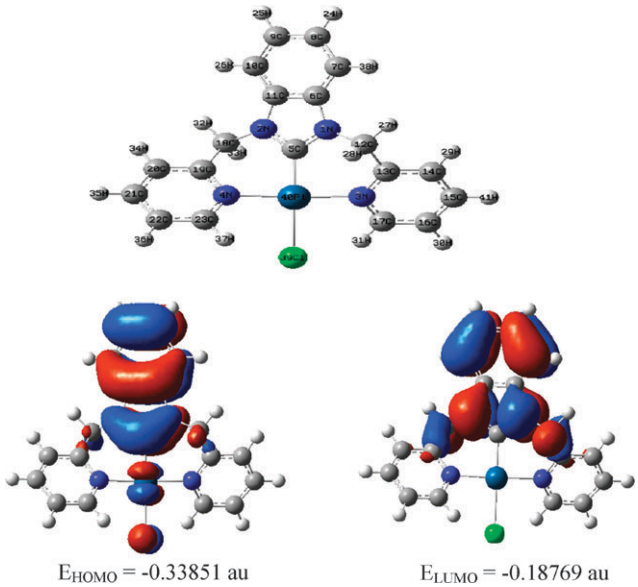

Fig. 3 The optimized structure and HOMO–LUMO orbitals of Pt(II) complex **3**.

Cyclic voltammetry studies were carried out using a Pt working electrode in acetonitrile with 0.1 M tetrabutylammonium hexafluorophosphate as the supporting electrolyte (shown in Fig. 4). The oxidation pattern of complex **2** shows a monoelectronic reversible process attributed to the Ru(II)/Ru(III) couple at 0.67 eV, which is less positive than the Ru(II)/Ru(III) couple for $Ru(bpy)_3^{2+}$ (1.29 V in dichloromethane) and for $Ru(tpy)_2^{2+}$ due to the strong electron donor properties of the NHC.[12j] On the other hand, complex **3** shows a bielectronic reversible process Pt(II)/Pt(IV) at 0.58 eV, which is less positive than in the case of [Pt(pbpy)Cl]Cl.[14b,c] The lower redox potential value of Pt-NHC **3** in comparison with Ru analog **2** is supported by the theoretically calculated ionization potential (0.3978908 *vs.* 0.429526 a.u.) and electron affinity (0.1381238 *vs.* 0.208874 a.u.) values (shown in Table 1).

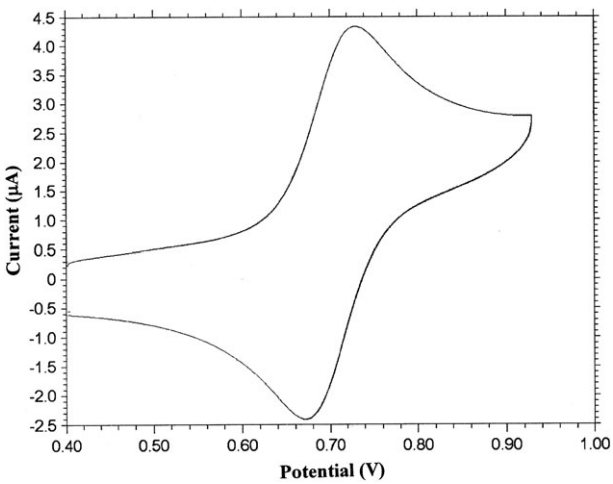

Fig. 4 The cyclic voltammogram of **2** in dry acetonitrile at a 100 mV s^{-1} scan rate with Pt as the working electrode, Ag/AgCl as the reference electrode and a 0.1 M solution of $[N(Bu)_4]PF_6$ as the supporting electrolyte.

Table 1 Theoretically calculated values of the ionisation potential (I), electron affinity (A), hardness (η), electronegativity (χ) and electrophilicity (ω)

Compound	I/a.u.	A/a.u.	η/a.u.	χ/a.u.	ω/a.u.
Ru(II) complex **2**	0.429526	0.208874	0.220652	0.3192	0.2309
Pt(II) complex **3**	0.3978908	0.1381238	0.259767	0.2680	0.1383

X-Ray structure of 2; comparison of bond parameters with theoretical values

Suitable single crystals of complex **2** were obtained by the slow diffusion of diethylether into a solution of **2** in acetonitrile. The asymmetric unit contained 33.33% acetonitrile. The crystal structure is shown in Fig. 4 and the crystal parameters are listed in Table 2.† The complex displays a coordination geometry very close to a perfect octahedron. The intraligand N–Ru–C angles range between 85.52 and 86.84°, whereas the interligand N–Ru–N angles have values from 85.61 to 93.87°. The two *trans*-carbenic ligands form an angle with the ruthenium atom very close to linearity (179.88°). This nearly perfect octahedron, is in contrast with the very distorted $[Ru(tpy)_2]^{2+}$ and $[Ru(bpy)_3]^{2+}$ complexes. The less distorted geometry in our case arises from the six-membered ring chelates. The flexible methylene bridge between the pyridine and the benzimidazole removes some of the strain of the complex.

As expected, the Ru–C bonds are shorter (2.020(5) and 2.025(5) Å) than the Ru–N bonds, which range between 2.099(4) and 2.120(3) Å. The Ru–C bonds are shorter than the similar Ru–N heterocyclic homoleptic biscarbene system (2.048–2.055 Å)[12j] and the biscarbene system (2.056–2.062 Å),[12k] whereas the Ru–N bond lengths are slightly longer in the present case than in similar biscarbene complexes (2.018–2.061 Å).[12j,k] The arrangement of the NCN ligands forms a double helix around the Ru(II) ion. Both enantiomers are found in the crystal packing, but this inherent chirality is in accordance with the diastereotopic effect observed for the CH_2 protons in the ^{1}H NMR spectrum.

Table 2 Crystallographic data for ligand **2**

	2
Empirical formula	$C_{43}H_{39.50}F_{12}N_{10.50}P_2Ru$
Formula weight	1094.35
Crystal system	Monoclinic
Space group	$P2_1/n$
T/K	200.0
Cell dimensions:	
a/Å	11.910(1)
b/Å	19.351(2)
c/Å	21.617(3)
α (°)	90.00
β (°)	90.20(1)
γ (°)	90.00
Volume/Å^3	4981.7(8)
Z	4
Density/Mg m^{-3}	1.459
Absorption coefficient (μ)	0.466
F(000)	2212.00
Crystal size/mm	0.10 × 0.16 × 0.38
Theta range for data collection	10–25
Index ranges	$-14 \le h \le 13$ $-22 \le k \le 22$ $-25 \le l \le 25$
Reflections collected	28 016
Independent reflections	7661
Max. and min. transmission	0.84, −0.54
Refinement method	$\bar{\varphi}$ and ω scans
TeXsan F refinement	5038
Observed data/restraints/parameters	5038/0/658
GOF	1.948
Final R indices [$I > 2\sigma(I)$]	0.12831
R indices (all data), wR	0.0632, 0.0659

Theoretical studies

To gain insight into the electronic situation of the synthesized complexes, we have performed theoretical calculations at the B3LYP/LANL2DZ level to compare the bond parameters of complexes **2** and **3**, as shown in Table 3 and Table 4. Electrophilicity, ionization potential, electron affinity, electronegativity and hardness can be considered preliminary tools for this purpose. Although it is unparallel to compare octahedral Ru(II) complex **2** with square planar Pt(II) complex **3**, the electrophilicity, ionization potential, electron affinity and electronegativity of the Ru(II) complex is higher than that of the Pt(II) complex, which reflects the experimentally determined redox potential. In the case of complex **2**, the theoretical results are in agreement with the experimental data obtained from the X-ray diffraction studies. The bond length values of complex **2** fit the experimental ones exceptionally well, whereas the bond angles deviate by between 2.8 and 0.1°. We did not succeed in obtaining single crystals of platinum complex **3**; however, theoretical calculations give a Pt–$C_{carbene}$ bond length of 1.954 Å, shorter than that previously reported for monocarbenes of between 1.981–2.072 Å.[18] The bond angles are in accordance with a square planar geometry (Table 4).

Experimental section

General procedures

All the reactions were carried out under nitrogen using standard Schlenk-type flasks. Work-up procedures were performed in air. All of the solvents and chemicals were purchased and used without further purification. The chemicals K_2PtCl_4, KPF_6, $AgPF_6$, picolylchloride hydrochloride, benzimidazole and $RuCl_3$ were purchased from Sigma-Aldrich, UK and Aurora Metthy, Kolkata. ^{1}H NMR and ^{13}C NMR spectra were recorded on a Bruker 400 spectrometer. Chemical shifts, δ in ppm, are reported to the internal standard TMS for both ^{1}H NMR and ^{13}C NMR. Microanalyses were performed on a Perkin-Elmer model 2400 instrument. Electronic absorption measurements were acquired with a Varian Cary 1 UV-vis spectrophotometer. Cyclic voltammetry was studied on a CH 600 analyzer using a platinum electrode as the working electrode, Ag/AgCl as the reference electrode and tetrabutylammonium hexafluorophosphate (0.1 M) as the supporting electrolyte in dry acetonitrile under an argon atmosphere at a 50 mV s^{-1} scan rate.

Synthesis of ligand 1

Synthesis of the ligand was reported earlier.[16] Benzimidazole (2 g, 16.94 mmol), 2-picolylchloride hydrochloride (2.77 g,

Table 3 Selected bond lengths (Å) and bond angles (°) for **2**

Experimental bond lengths	Theoretical bond lengths[a]	Experimental bond angles	Theoretical bond angles[a]
Ru–N3 = 2.102(4)	Ru–N3 = 2.102	N3–Ru1–N4 = 172.2(2)	N3–Ru1–N4 = 172.2
Ru–N4 = 2.099(4)	Ru–N4 = 2.099	N3–Ru1–N7 = 93.9(2)	N3–Ru1–N7 = 93.1
Ru–N7 = 2.103(4)	Ru–N7 = 2.102	N3–Ru1–N8 = 85.6(1)	N3–Ru1–N8 = 88.4
Ru–N8 = 2.120(4)	Ru–N8 = 2.120	N3–Ru1–C1 = 86.8(2)	N3–Ru1–C1 = 85.5
Ru–C1 = 2.020(5)	Ru–C1 = 2.021	N3–Ru1–C2 = 93.0(2)	N3–Ru1–C2 = 94.6
Ru–C2 = 2.025(5)	Ru–C2 = 2.025	N4–Ru1–N7 = 88.4(2)	N4–Ru1–N7 = 85.6
		N4–Ru1–N8 = 93.1(2)	N4–Ru1–N8 = 93.9
		N4–Ru1–C1 = 85.6(2)	N4–Ru1–C1 = 86.8
		N4–Ru1–C2 = 94.6(2)	N4–Ru1–C2 = 93.1
		N7–Ru1–N8 = 172.5(2)	N7–Ru1–N8 = 172.5
		N7–Ru1–C1 = 93.6(2)	N7–Ru1–C1 = 93.6
		N7–Ru1–C2 = 86.3(2)	N7–Ru1–C2 = 86.3
		N8–Ru1–C1 = 93.8(2)	N8–Ru1–C1 = 93.8
		N8–Ru1–C2 = 86.3(2)	N8–Ru1–C2 = 86.2
		C1–Ru1–C2 = 179.8(2)	C1–Ru1–C2 = 179.9

[a] Theoretically calculated bond parameters at the B3LYP/LANL2DZ level.

Table 4 Theoretically calculated bond parameters of **3** at the B3LYP/LANL2DZ level

Theoretical bond lengths/Å	Theoretical bond angles (°)
Pt–N3 = 2.078	C(1)–Pt–N4 = 88.58
Pt–N4 = 2.078	C(1)–Pt–N5 = 88.56
Pt–Cl = 2.454	Cl–Pt–N4 = 91.44
Pt–C(1) = 1.954	Cl–Pt–N5 = 91.42
	N2–C(1)–N3 = 107.91
	N3–Pt–N4 = 177.14
	Cl–Pt–C(1) = 179.97

23.6 mmol) and $NaHCO_3$ (4.27 g, 50.8 mmol) were stirred in 60 mL EtOH and refluxed for 3 d. The solvent was then removed, and the gummy mass treated with 50 mL dichloromethane and filtered to remove the NaCl and excess $NaHCO_3$. Finally, the volume of the reddish solution was reduced to 10 mL and added to cold Et_2O to obtain a light solid mass. The yield was 60%.

^{1}H NMR (400 MHz, CD_3CN, 25 °C): δ 10.43 (s, 1H, NCHN), 8.40 (d, 2H, J = 4.56 Hz, pyridine-C4H), 7.77–7.73 (m, 4H, Ar–H and pyridine C5), 7.57 (d, 2H, J = 7.87, pyridine-C6H), 7.51 (m, 2H, pyridine-C3H), 7.24 (m, 2H, Ar–H), 5.83 (s, 4H, NCH_2-benzimidazole). ^{13}C NMR (400 MHz, CD_3CN, 25 °C): δ 152.2 (C2-pyridine), 150.1 (C5-pyridine), 142.5 (NCN), 139.3 (C4-pyridine), 133.2, 126.6 (Ar-C), 125.4 (C3-pyridine), 124.3 (C6-pyridine), 114.5 (Ar-C), 52.4 (NCH_2-benzimidazole). Anal. calc. for $C_{19}H_{17}N_4Cl{\cdot}H_2O$: C, 64.31; H, 5.35; N, 15.79. Found: 63.71; H, 4.38; N, 15.54%.

Synthesis of Ru(II) complex 2

A mixture of $RuCl_3{\cdot}3H_2O$ (0.1 g, 0.44 mmol), ligand **1** (0.2 g, 0.87 mmol) and K_2CO_3 (0.2 g, 1.31 mmol) in 5 mL ethyleneglycol was heated at 160 °C for 6 h. The resulting solution became dark brown-red, was left to cool for 1 h and transferred to a 250 mL beaker. To this solution was added a saturated solution of KPF_6, and a greenish-yellow precipitate was observed. The precipitate was dried and purified by column chromatography. The orange-red mass was eluted in $CHCl_3$–CH_3CN (2 : 1). The product was recrystallised from acetonitrile and diethylether. The yield was 65%.

λ_{max}^{abs} = 386 nm in acetonitrile. ^{1}H NMR (400 MHz, CD_3CN, 25 °C): δ 7.91 (m, 2H, C_4H-py), 7.68 (d, 4H, J = 4.04 Hz, $C_{3,6}$H-py), 7.52 (m, 2H, C_5H-py), 7.28 (d, 2H, J = 6.0 Hz, Ph-H), 6.69 (m, 2H, Ph-H), 5.87 (d, 2H, J = 15.56 Hz, N–CH_2–py), 4.79 (d, 2H, J = 16.04 Hz, N–CH_2–py). ^{13}C NMR (400 MHz, CD_3CN, 25 °C): δ 207.0 (NCN), 158.2, 157.5 (C2-pyridine), 137.6 (C6-pyridine), 134.8 (C6-pyridine), 126.8 (C3-pyridine), 125.0 (C4-pyridine), 122.9 (C5-pyridine), 110.1, 50.5 (NCH_2-benzimidazole). Anal. calc. for $C_{38}H_{32}N_8RuP_2F_{12}$: C, 46.00; H, 3.22; N, 11.30. Found: C, 45.44; H, 3.33; N, 11.12%.

Synthesis of Pt(II) complex 3

Ligand **1** (0.2 g, 0.50 mmol) and Ag_2O (0.05 g, 0.25 mmol) were dissolved in 10 mL DMSO and the solution stirred in the dark for 5 h. The silver carbene was added dropwise to a 5 mL yellow solution of K_2PtCl_4 (0.2 g, 0.50 mmol) in the dark at rt. Next, the resulting solution was heated for 2 h at 90 °C. During this time, the color of the solution changed from yellow to white. After $AgPF_6$ (0.12 g, 0.50 mmol) had been added, the resulting mixture was stirred under cold conditions for another 30 min. The cold solution was filtered through G-4 sinter glass. The solution was diluted by the addition of 25 mL of dichloromethane. About 250 mL of diethylether was added to the diluted solution obtain a colourless precipitate. The precipitate was filtered and washed several times with diethylether. The colourless solid was dried *in vacuo*. The yield was 75%.

^{1}H NMR (CD_3CN, 25 °C): δ 9.62 (d, 2H, J = 7.04 Hz, C_6H-py), 8.16 (t, 2H, J = 3.76 Hz, C_3H-py), 7.91 (d, 2H, J = 9.04 Hz, C_5H-benzimidazole), 7.84 (m, 4H, C_4H-py), 7.58 (t, 2H, J = 3.56 Hz, C_5H-py), 7.55 (m, 2H, J = 4.4 Hz, $C_{6,7}$H-benzimidazole), 5.61 (d, 2H, J = 15.56 Hz, N–CH_2–py), 5.44 (d, 2H, J = 15.56 Hz, N–CH_2–py). ^{13}C NMR (400 MHz, CD_3CN, 25 °C): δ 207.0 (NCN), 158.2, 157.5 (C2-pyridine), 137.6 (C6-pyridine), 134.8 (C6-pyridine), 126.8 (C3-pyridine), 125 (C4-pyridine), 122.9 (C5-pyridine), 110.1, 50.5 (N–CH_2–benzimidazole). Anal. calc. for $C_{19}H_{16}N_4PtClPF_6$: C, 33.74; H, 2.37; N, 8.29. Found: C, 32.98; H, 2.58; N, 8.09%. Mass (ESI): m/z = 531.1 $[M - PF_6]^+$.

Computational details

The geometries of the Ru(II) and Pt(II) complexes were optimized at the B3LYP/LANL2DZ level of theory using the Gaussian 03W[19] program. The number of imaginary frequencies of all the molecules turned out to be zero, implying that they correspond to minimum energy structures on the potential energy surface. The frontier molecular orbitals of these complexes were generated in Gaussview using the same level of theory. The conceptual density functional theory based on global reactivity descriptors like electronegativity (χ),[20] hardness (η)[21] and electrophilicity (ω)[22] was also calculated. After obtaining ionisation potential (I) and electron affinity (A) values using the ΔSCF [$I = E(N-1) - E(N)$ and $A = E(N) - E(N+1)$] technique, the hardness was calculated using the equation $\eta = I - A$. The global electrophilicity index (ω) was calculated from the explicit formula [$\omega = \chi^2/2\eta$], involving the electronegativity and hardness proposed by Parr and Pearson.[21] The frontier molecular orbitals were generated using GV03 at the same level of theory.

X-Ray structure determination

X-Ray diffraction data were collected using an Enraf Nonius kappa CCD detector. Crystal data collection and refinement parameters are summarized in Table 2. The structure was refined on F using the 'Full' matrix type and solved by the TeXsan[23] programme.†

Conclusion

Terpyridine (tpy) and phenylbipyridine (pbpy) bis-homoleptic octahedral Ru(II) and square planar Pt(II) complexes of the ligand 1,3-bis(2-pyridylmethyl)-1*H*-benzimidazolium chloride have been synthesized and fully characterized by different spectroscopic techniques. The solid state X-ray crystal structure of the Ru(II) complex showed a distorted octahedral geometry. Due to unavailability of single crystals of the square planar Pt(II) complex, the structure was by optimized using the Gaussian 03W program. Both of the platinum group metal complexes were non-emmissive in acetonitrile, although the corresponding tpy and pbpy complexes were promisingly luminescent. Electrochemical studies of the complexes showed the Ru(II)/Ru(III) couple and Pt(II)/Pt(III) couple at 0.67 and 0.58 eV, respectively, which are lower potentials than the π-acidic ligands bpy, tpy and pbpy, which also supports the better σ-donor properties of NHCs. Beyond the complexes' synthesis and characterization, theoretical calculations were performed to compare with and support with experiment results, and to explain their photoelectronic and electrochemical properties. The estimation of the catalytic and DNA binding activities of complex **3** is under way.

Acknowledgements

JD thanks the Department of Science and Technology, DST, India for financial support under 'SERC Fast Track Young Scientist Scheme' (SR/FT/CS-046/2009) and the Haldia Institute of Technology for lab space. We are also grateful to the referees for their valuable comments during the review process.

References.

1 A. J. Arduengo, III, R. L. Harlow and M. A. Kline, *J. Am. Chem. Soc*., 1991, **113**, 361–363.
2 (*a*) F. E. Hahn, *Angew. Chem., Int. Ed*., 2006, **45**, 1348–1352; (*b*) W. A. Herrmann, *Angew. Chem., Int. Ed*., 2002, **41**, 1290–1309; (*c*) D. Bourissou, O. Guerret, F. P. Gabbai and G. Bertrand, *Chem. Rev*., 2000, **100**, 39–92; (*d*) W. A. Herrmann and C. Köcher, *Angew. Chem., Int. Ed. Engl*., 1997, **36**, 2162–2187.
3 (*a*) F. E. Hahn and M. C. Jahnke, *Angew. Chem*., 2008, **120**, 3166–3179; (*b*) *Recent Developments in the Organometallic Chemistry of* N-*Heterocyclic Carbenes*, ed. R. H. Crabtree, 2000; (*c*) *N*-Heterocyclic Carbenes in Transition Metal Catalysis, *Top. Organomet. Chem*., ed. F. Glorius, 2007, vol. 21, pp. 1–218; (*d*) N. Marion, S. Díez-González and S. P. Nolan, *Angew. Chem*., 2007, **119**, 3046–3050 (*Angew. Chem., Int. Ed*., 2007, **46**, 2988–3000).
4 (*a*) M. Albrecht and G. van Koten, *Angew. Chem., Int. Ed*., 2001, **40**, 3750–3781; (*b*) D. Olsson, P. Nilsson, M. E. Masnaouy and O. F. Wendt, *Dalton Trans*., 2005, 1924; (*c*) D. Morales-Morales, C. Grause, K. Kasaoka, R. Redon, R. E. Cramer and C. M. Jensen, *Inorg. Chim. Acta*, 2000, **300–302**, 958–986; (*d*) D. Morales-Morales, R. Redon, C. Yung and C. M. Jensen, *Chem. Commun*., 2000, 1619–1620; (*e*) M. R. Eberhard, *Org. Lett*., 2004, **6**, 2125–2128; (*f*) D. S. McGuinness and K. J. Cavell, *Organometallics*, 2000, **19**, 741–748.
5 (*a*) W. A. Herrmann and C. Kocher, *Angew. Chem., Int. Ed. Engl*., 1997, **36**, 2162–2187; (*b*) W. A. Herrmann, *Angew. Chem., Int. Ed*., 2002, **41**, 1290–1309.
6 (*a*) A. J. Arduengo, III, *Acc. Chem. Res*., 1999, **32**, 913–921; (*b*) W. A. Herrmann and C. Kochner, *Angew.Chem.Int.edn*, 1997, **36**, 2163–2187; (*c*) E. Peris and R. H. Crabtree, *Coord. Chem. Rev*., 2004, **248**, 2239–2246; (*d*) C. M. Crudden and D. P. Allan, *Coord. Chem. Rev*., 2004, **248**, 2247–2273; (*e*) D. Pugh and A. A. Danopoulos, *Coord. Chem. Rev*., 2007, **251**, 610–641 and references therein.
7 (*a*) K. J. Cavell and D. S. McGuinness, *Coord. Chem. Rev*., 2004, **248**, 671–681; (*b*) W. A. Herrmann, *Angew. Chem., Int. Ed*., 2002, **41**, 1290–1309; (*c*) E. Peris and R. H. Crabtree, *Coord. Chem. Rev*., 2004, **248**, 2239–2246; (*d*) M. D. Sanderson, J. W. Kamplain and C. W. Bielawski, *J. Am. Chem. Soc*., 2006, **128**, 16514–16515; (*e*) C. D. Varnado Jr, V. M. Lynch and C. W. Bielawski, *Dalton Trans*., 2009, 7253–7261 and references therein.
8 (*a*) F. Guillen, C. L. Winn and A. Alexakis, *Tetrahedron: Asymmetry*, 2001, **12**, 2083–2208; (*b*) R. H. Crabtree, *J. Organomet. Chem*., 2005, **690**, 5451–5457; (*c*) E. Peris, J. Mata, J. A. Loch and R. H. Crabtree, *Chem. Commun*., 2001, 201–202; (*d*) J. R. Miecznikowski, S. Gruendemann, M. Albrecht, C. Megret, E. Clot, J. W. Faller, O. Eisenstein and R. H. Crabtree, *Dalton Trans*., 2003, 831–838; (*e*) B. Wang, D. Wang, D. Cui, W. Gao, T. Tang, X. Chen and X. Jing, *Organometallics*, 2007, **26**, 3167–3172.
9 S. Leuthäußer, D. Schwarz and H. Plenio, *Chem.–Eur. J*., 2007, **13**, 7195–7203.
10 (*a*) J. C. C. Chen and I. J. B. Lin, *J. Chem. Soc., Dalton Trans*., 2000, 839–840; (*b*) D. Pugh and A. A. Danopoulos, *Coord. Chem. Rev*., 2007, **251**, 610–641; (*c*) D. J. Nielsen, K. J. Cavell, B. W. Skelton and A. H. White, *Inorg. Chim. Acta*, 2002, **327**, 116–125.
11 (*a*) A. A. D. Tulloch, A. A. Danopoulos, R. P. Tooze, S. M. Cafferkey, S. Kleinhenz and M. B. Hursthouse, *Chem. Commun*., 2000, 1247–1248; (*b*) F. E. Hahn, M. C. Jahnke, V. Gomez-Benitez, D. Morales-Morales and T. Pape, *Organometallics*, 2005, **24**, 6458–6463; (*c*) F. E. Hahn, C. Holtgrewe, T. Pape, M. Martin, E. Sola and L. A. Oro, *Organometallics*, 2005, **24**, 2203–2209; (*d*) F. E. Hahn, M. C. Jahnke and T. Pape, *Organometallics*, 2007, **26**, 150–154.
12 (*a*) D. S. McGuinness, V. C. Gibson, D. F. Wass and J. W. Steed, *J. Am. Chem. Soc*., 2003, **125**, 12716–12717; (*b*) J. A. Wright, S. Freeman and A. A. Danopoulos, *Dalton Trans*., 2006, 775–782; (*c*) S. Gründemann, M. Albrecht, J. A. Loch, J. W. Faller and

R. H. Crabtree, *Organometallics*, 2001, **20**, 5485–5488; (*d*) A. A. D. Tulloch, A. A. Danopoulos, G. J. Tizzard, S. L. Coles, M. B. Hursthouse and R. S. Hay-Motherwell, *Chem. Commun.*, 2001, 1270–1271; (*e*) A. A. Danopoulos, N. Tsoureas, J. A. Wright and M. E. Light, *Organometallics*, 2004, **23**, 166–168; (*f*) K. Inamoto, J. Kuroda, K. Hiroya, Y. Noda, M. Watanabe and T. Sakamoto, *Organometallics*, 2006, **25**, 3095–3098; (*g*) A. A. Danopoulos, J. A. Wright, W. B. Motherwell and S. Ellwood, *Organometallics*, 2004, **23**, 4807–4810; (*h*) D. S. McGuinness, V. C. Gibson and J. W. Steed, *Organometallics*, 2004, **23**, 6288–6292; (*i*) E. Masllorens, M. Rodríguez, I. Romero, A. Roglans, T. Parella, J. Benet-Buchholz, M. Poyatos and A. Llobet, *J. Am. Chem. Soc.*, 2006, **128**, 5306–5307; (*j*) S. U. Son, K. H. Park, Y. Lee, B. Y. Kim, C. H. Choi, M. S. Lah, Y. H. Jang, D. Jang and Y. K. Chung, *Inorg. Chem.*, 2004, **43**, 6896–6898; (*k*) M. Poyatos, J. A. Mata, E. Falomir, R. H. Crabtree and E. Peris, *Organometallics*, 2003, **22**, 1110–1114; (*l*) A. A. Danopoulos, S. Winston and W. B. Motherwell, *Chem. Commun.*, 2002, 1376–1377; (*m*) J. A. Wright, A. A. Danopoulos, Motherwell, R. J. Carroll and S. Ellwood, *J. Organomet. Chem.*, 2006, **691**, 5204–5210.

13 (*a*) W. M. Xue, M. C.-W. Chan, Z.-M. Su, K.-K. Cheung, S.-T. Liu and C.-M. Che, *Organometallics*, 1998, **17**, 1622–1630; (*b*) Q.-X. Liu, F.-B. Xu, Q.-S. Li, X.-S. Zeng, X.-B. Leng, Y. L. Chou and Z.-Z. Zhang, *Organometallics*, 2003, **22**, 309–314; (*c*) S. U. Son, K. H. Park, Y.-S. Lee, B. Y. Kim, C. H. Choi, M. S. Lah, Y. H. Jang, D.-J. Jang and Y. K. Chung, *Inorg. Chem.*, 2004, **43**, 6896–6898.

14 (*a*) W. G. Holthoff, E. C. Tehan, R. M. Bukowski, N. Kent, B. D. MacCraith and F. V. Bright, *Anal. Chem.*, 2005, **77**, 718–723; (*b*) S.-W. Lai, M. C.-W. Chan, K.-K. Cheung and C.-M. Che, *Organometallics*, 1999, **18**, 3327–3336; (*c*) S.-W. Lai, H.-W. Lam, W. Lu, K.-K. Cheung and C.-M. Che, *Organometallics*, 2002, **21**, 226–234; (*d*) J. Schneider, P. Du, P. Jarosz, T. Lazarides, X. Wang, W. W. Brennessel and R. Eisenberg, *Inorg. Chem.*, 2009, **48**, 4306–4316.

15 (*a*) J. Brooks, Y. Babayan, S. Lamansky, P. I. Djurovich, I. Tsyba, R. Bau and M. E. Thompson, *Inorg. Chem.*, 2002, **41**, 3055–3066; (*b*) D.-L. Ma, C.-M. Che and S.-C. Yan, *J. Am. Chem. Soc.*, 2009, **131**, 1835–1846; (*c*) J. B. Waern, C. Desmarets, L.-M. Chamoreau, H. Amouri, A. Barbieri, C. Sabatini, B. Ventura and F. Barigelletti, *Inorg. Chem.*, 2008, **47**, 3340–3348.

16 S. U. Son, K. H. Park, Y.-S. Lee, B. Y. Kim, C. H. Choi, M. S. Lah, Y. H. Jang, D.-J. Jang and Y. K. Chung, *Inorg. Chem.*, 2004, **43**, 6896–6898.

17 (*a*) J. C. C. Chen and I. J. B. Lin, *Organometallics*, 2000, **19**, 5113–5121; (*b*) H. M. J. Wang, C. S. Vasam, T. Y. R. Tsai, S.-H. Chen, A. H. H. Chang and I. J. B. Lin, *Organometallics*, 2005, **24**, 486–493; (*c*) X. Hu and K. Meyer, *J. Organomet. Chem.*, 2005, **690**, 5474–5484; (*d*) X. Hu, I. Castro-Rodriguez and K. Meyer, *Chem. Commun.*, 2004, 2164–2165; (*e*) X. Hu, Y. Tang, P. Gantzel and K. Meyer, *Organometallics*, 2003, **22**, 612–614; (*f*) D. J. Nielsen, K. J. Cavell, B. W. Skelton and A. H. White, *Inorg. Chim. Acta*, 2002, **327**, 116–126; (*g*) C. P. Newman, R. J. Deeth, G. J. Clarkson and J. P. Rourke, *Organometallics*, 2007, **26**, 6225–6233.

18 (*a*) G. Berthon-Gelloz, O. Buisine, J.-F. Brière, G. Michaud, S. Stérin, G. Mignani, B. Tinant, J.-P. Declercq, D. Chapon and I. E. Markó, *J. Organomet. Chem.*, 2005, **690**, 6156–6168; (*b*) M. A. Duin, M. Lutz, A. L. Spek and C. J. Elsevier, *J. Organomet. Chem.*, 2005, **690**, 5804–5815; (*c*) S. Fantasia, J. L. Petersen, H. Jacobsen, L. Cavallo and Steven P. Nolan, *Organometallics*, 2007, **26**, 5880–5889.

19 M. J. Frisch, G. W. Trucks, H. B. Schlegel, G. E. Scuseria, M. A. Robb, J. R. Cheeseman, J. A. Montgomery, Jr., T. Vreven, K. N. Kudin, J. C. Burant, J. M. Millam, S. S. Iyengar, J. Tomasi, V. Barone, B. Mennucci, M. Cossi, G. Scalmani, N. Rega, G. A. Petersson, H. Nakatsuji, M. Hada, M. Ehara, K. Toyota, R. Fukuda, J. Hasegawa, M. Ishida, T. Nakajima, Y. Honda, O. Kitao, H. Nakai, M. Klene, X. Li, J. E. Knox, H. P. Hratchian, J. B. Cross, V. Bakken, C. Adamo, J. Jaramillo, R. Gomperts, R. E. Stratmann, O. Yazyev, A. J. Austin, R. Cammi, C. Pomelli, J. Ochterski, P. Y. Ayala, K. Morokuma, G. A. Voth, P. Salvador, J. J. Dannenberg, V. G. Zakrzewski, S. Dapprich, A. D. Daniels, M. C. Strain, O. Farkas, D. K. Malick, A. D. Rabuck, K. Raghavachari, J. B. Foresman, J. V. Ortiz, Q. Cui, A. G. Baboul, S. Clifford, J. Cioslowski, B. B. Stefanov, G. Liu, A. Liashenko, P. Piskorz, I. Komaromi, R. L. Martin, D. J. Fox, T. Keith, M. A. Al-Laham, C. Y. Peng, A. Nanayakkara, M. Challacombe, P. M. W. Gill, B. G. Johnson, W. Chen, M. W. Wong, C. Gonzalez and J. A. Pople, *GAUSSIAN 03 (Revision B.03)*, Gaussian, Inc., Wallingford, CT, 2004.

20 (*a*) P. K. Chattaraj, *J. Indian Chem. Soc.*, 1992, **69**, 173–183; (*b*) R. G. Parr, R. A. Donnelly, M. Levy and W. E. Palke, *J. Chem. Phys.*, 1978, **68**, 3801–3807.

21 (*a*) R. G. Parr and R. G. Pearson, *J. Am. Chem. Soc.*, 1983, **105**, 7512–7516; (*b*) R. G. Pearson, *Chemical Hardness: Applications from Molecules to Solids*, Wiley-VCH, Weinheim, 1997.

22 (*a*) R. G. Parr, L. v. Szentpaly and S. Liu, *J. Am. Chem. Soc.*, 1999, **121**, 1922–1924; (*b*) P. K. Chattaraj, U. Sarkar and D. R. Roy, *Chem. Rev.*, 2006, **106**, 2065–2091; (*c*) P. K. Chattaraj and D. R. Roy, *Chem. Rev.*, 2007, **107**, PR46–PR74.

23 *TeXsan version 1.7: single crystal structure analysis software*, Molecular Structure Corporation, The Woodlands, Texas, USA, 1992–1997.

